



DISCLAIMER: More detailed information on the results and/or performance obtained and their use is available in the Subproject's subsequent Deliverable (D2.3.4) and/or Periodic Report.

Project Number:	604102	Project Title:	Human Brain Project
Document Title:	Strategic Human Data for the HBP Human Brain Atlas: Package one (data)		
Document Filename:	SP2 D2.3.3 FINAL		
Deliverable Number:	D2.3.3		
Deliverable Type:	Data		
Work Package(s):	WPs 2.2.1, 2.2.2		
Dissemination Level:	PU = Public		
Planned Delivery Date:	M19/30 April 2015		
Actual Delivery Date:	M25/20 Oct 2015		
Authors:	Katrin AMUNTS, JUELICH/UDUS		
Compiling Editors:	Angela LINDNER, UDUS, Timo DICKSCHEID, JUELICH		
Contributors:	Jeff MANGIN, CEA Cyril Poupon, CEA Javier DEFELIPE, UPM Simon EICKHOFF, JUELICH/UDUS Ghislaine DEHAENE, CEA Hartmut MOHLBERG, JUELICH Karl ZILLES, JUELICH Markus AXER, JUELICH Nicole SCHUBERT, JUELICH Bertrand THIRION, INRIA Jean-Philippe LACHAUX, UCBL Francesco PAVONE, LENS Huib MANSVELDER, VU		
STO Review:	UHEI (P45): Sabine SCHNEIDER		
Editorial Review:	EPFL (P1): Guy WILLIS, Lauren ORWIN		
Abstract:	<p>This report describes the first package of multi-level human brain data as it was delivered to the HBP Brain Atlas. The different kinds of data, their provenance and the format in which they were delivered to the Collaboratory (formerly Unified Portal) are described in detail. Strategic methods for providing data are also described.</p>		
Keywords:	<p>Data and tools for the HBP Brain Atlas, multi-level <i>post mortem</i> and <i>in vivo</i> human brain data, tools to integrate data into HBP atlas</p>		



Table of Contents

1. Introduction	4
2. Strategic Human Data for the HBP Human Brain Atlas	5
2.1 Whole Human Brain Cytoarchitectonic and Maximum Probability Maps (Eickhoff, Mohlberg, JUELICH)	5
2.2 Numbers and Distributions of Neurons and Glia (DeFelipe, UPM)	7
2.3 High resolution whole brain volumetric data; BigBrain (Mohlberg, JUELICH)	8
2.4 Morphologies of selected neurons (Mansvelder, VU)	8
2.5 Quantitative Receptor data (Zilles, JUELICH)	9
2.6 <i>In vivo</i> fibre tract scans and diffusion-based data on major and U-shaped tracts (Mangin, Poupon, CEA)	9
2.7 Wistar rat brain fibre orientation model (Axe, Schubert, JUELICH)	16
2.8 Whole rat brain receptor data (Schubert, Zilles, JUELICH)	17
2.9 Infant atlas and major tracts in infant brains (Dehaene-Lambertz, CEA)	18
2.10 Human Intracranial Database (Lachaux, UCLB)	18
2.11 High-resolution optical imaging of human brain (Pavone, LENS)	19
3. Strategic Methods for the HBP Human Brain Atlas	19
3.1 Individual brain charting and meta-analysis (Thirion, INRIA)	19
3.2 SPM Anatomy Toolbox (Eickhoff)	21
3.3 A cross modality alignment toolbox based on sulci (Mangin)	21
Annex A: References	23
Annex B: Data set Identification Card	25
Annex C: Receptor binding site densities for selected areas	26
Annex D: JuBrain Ontology used in cytoarchitectonic atlas with direct relationship to Allen Brain Atlas	28



List of Figures

Figure 1: Examples of anatomical allocation by the JuBrain cytoarchitectonic atlas for heterogeneous types of cognitive neuroscience datasets..... 5

Figure 2: Segmentation of the long white matter bundles obtained for all the subjects of the CONNNECT/Archi database. 12

Figure 3: Examples of individual tractograms, segmented long and short white matter bundles, density map, quantitative diffusion map, and quantitative T1 relaxation time..... 13

Figure 4: Representation of the atlas of long white matter connectivity merging the fibres of all the subjects, and example of bundle probability density maps, as well as atlases of quantitative diffusion and relaxometry indices. 15

Figure 5: Example of the T2* image (left), the delineated atlas image (middle), and the fibre orientation map (right) of a coronal rat brain section in the same sectioning plane..... 16

Figure 6: This 3D model in the stereotaxic reference space facilitates a multimodal voxel-wise analysis of the distribution of the receptors in 3D..... 18

Figure 7: Applied to a corpus of 30 studies that we have gathered, our meta-analytic approach enables us to automatically and objectively map 20 cognitive terms. We report the corresponding regions for each concept in the above figure (Schwartz et al., submitted). 20

List of Tables

Table 1: Provision of data on different cell types in different cortical areas..... 7

Table 2: Cortical areas according to the JuBrain nomenclature and subcortical regions with mean \pm s.d. receptor binding site densities in fmol/mg protein in five adult human brains. 27



1. Introduction

Aim of this document:

This report describes the first package of multi-level data and related tools that are ready for HBP-internal integration in the HBP brain atlas as scheduled for Month18. The datasets are described in detail in the following chapters, including information about their role in the atlas, provenance, and the way they are being delivered to the brain atlas (Collaboratory, ex-Unified Portal) or shared with other SPs.

Brief overview of data and its scientific significance

The data in this first package already covers a wide spectrum of modalities and scales for the human brain. It includes the ultra high-resolution BigBrain Model, showing optical densities based on cells on an impressive isotropic resolution of 20 micron in 3D. An initial parcellation of the auditory cortex has been natively mapped in the Big Brain space, and is exclusively provided to the HBP atlas.

Microstructural data also includes measurements of densities of different types of cells in ~20 different cortical areas, and measurements for fifteen ligands in three primary sensory, the primary motor, 11 higher associative cortical areas, putamen, globus pallidus and two thalamic nuclei, covering major receptor types of classical neurotransmitters as well as adenosine.

On the macroscale, the delivery includes new versions of the JuBrain maximum probability and probabilistic maps, a complete atlas template of a human infant containing 3D surface meshes of approximately 50 regions, and probabilistic atlases and 3D meshes for 30 deep white matter bundles

An important step to link cytoarchitecture with gene expressions has been taken by providing a detailed ontology for the JuBrain cytoarchitectonic Atlas, corresponding to that of the Allen atlas (see next paragraph).

Brief description of how the data link to the Neuroinformatics and other Platforms

The JuBrain Dataset and the BigBrain Datasets have been transferred and registered into the HBP portal in collaboration with SP5. The Data are qualitatively complete and represent the most up to date version.

The JuBrain ontology, the data on neuronal cell distribution and receptor distributions is delivered to SP5 as Excel sheets with quantitative data linked to the ontology (Annex E, Table 1).

Data from *in vivo* fibre tract scans and diffusion-based data on major and U-shaped tracts are delivered in NIFTI resp. in BrainVISA and VTK formats.

The entire data set of aligned FOM (fibre orientation model) is assembled and being delivered in a single NIFTI file.

Data from neuronal recordings have been shared continuously with partners in SP4 and SP6 to populate models of synapses, neurons and networks of neurons with accurate morphological and physiological parameters. A reference dataset including digitally reconstructed neurons with matching physiological data from these neurons, as well as morphologies and physiologies of synaptically connected neuron pairs have been exchanged with SPs 4 and 6.

2. Strategic Human Data for the HBP Human Brain Atlas

2.1 Whole Human Brain Cytoarchitectonic and Maximum Probability Maps (Eickhoff, Mohlberg, JUELICH)

2.1.1 Data Description

The JuBrain cytoarchitectonic atlas consists of probabilistic maps for human brain structures defined by histological analysis of ten post-mortem brains. The individual maps are furthermore combined into a Maximum Probability Map that assigns each voxel in the brain to the most likely histological area at that particular position. This cytoarchitectonic atlas is a key element of the HBP Human Brain Atlas, representing the most detailed structural parcellation of the cortex currently available. It is of utmost relevance for functional and cognitive neuroscientists to localise their findings and activations patterns in a common structural framework, and thus helps bridge the gap between function and structure by allowing an objective integration of *in-vivo* data with histological findings, using quantitative tools (Eickhoff *et al.*, 2005, 2007).

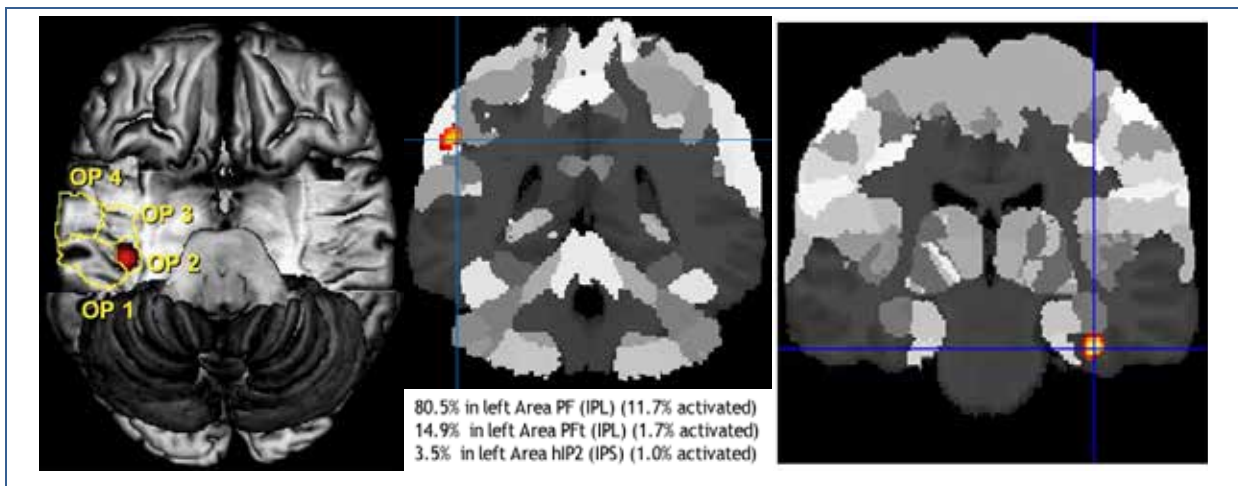


Figure 1: Examples of anatomical allocation by the JuBrain cytoarchitectonic atlas for heterogeneous types of cognitive neuroscience datasets.

Left: Localisation of the human vestibular cortex as identified through a meta-analysis of 28 neuroimaging experiments to histological area OP 2 on the parietal operculum (zu Eulenburg *et al.*, 2012). **Middle:** Cytoarchitectonic assignment of a parietal region showing neuropsychological-morphometric correlation with executive motor control in a sample of 397 healthy subjects (Genon *et al.*, in preparation). **Right:** Findings showing that contrary to common belief, it is not the hippocampus, but rather the parahippocampal gyrus that shows increased connectivity in patients with auditory-verbal hallucinations (Sommer *et al.*, 2012).

To date, the atlas contains 60 structures. These are ready for a public data release, since they have all been described and published in peer-reviewed journals. For roughly the same number of additional structures, histological mapping has already been completed, but the data has not yet been completely analysed published. Finally, around 90 further structures are currently being mapped.

Deposition of this data into the Neuroinformatics Platform (NIP) was part of the work in Task 2.2.2. The dataset has now been transferred and registered (registration ID 5f160654-0e7f-11e5-9b89-6003088da632) and can be accessed via the following url: <https://nip.humanbrainproject.eu/observation.html?id=5f160654-0e7f-11e5-9b89-6003088da632> . Until now, transfer and registration have been carried out by direct communication between SP2 and SP5 (FTP, e-mail, existing academic cloud storage).

Along with the datasets, SP2 has created a detailed table of the JuBrain ontology used in the cytoarchitectonic atlas. This also establishes a direct relationship with the ontology of



the Allen Human Brain Atlas¹, which is of potential interest for the neuroscience community. The ontology table has been handed out as an Excel sheet to SP5 for HBP-internal release and integration into the knowledge graph, and is attached in the appendix of this Deliverable (Appendix E; reference <https://www.jubrain.fz-juelich.de/apps/cytoviewer/cytoviewer.php>). Together with the cytoarchitectonic atlas, it allows the implementation of a tree-like navigation from macroanatomical to cytoarchitectonic structures in the HBP portal as a next step.

The cytoarchitectonic probabilistic and maximum probability maps deposited in the HBP portal represent the most up-to-date version of this data. The deposited version of the JuBrain cytoarchitectonic human brain maps is provided in the standard MNI single subject template space, and will be supplemented in the future by a version of the atlas transformed to the MNI-ICBM152nlin2009casym space, a widely accepted averaged brain template. The deposition is thus in accordance with the deliverable planned for Month 18.

2.1.2 Data Provenance

The cytoarchitectonic maps are based on observer-independent histological mapping performed in 10 human post-mortem brains. These brains were obtained via the body donor programme of the Department of Anatomy at the University of Düsseldorf, Germany, as approved by the local ethics committee. Details on the histological processing have been extensively described in peer-reviewed publications (e.g., Amunts *et al.*, 1999, 2004; Zilles *et al.*, 2002), the approach for observer-independent delineation of brain regions is summarised in (Zilles *et al.*, 2002; Schleicher *et al.*, 2005) and detailed specifically for each particular brain structure in the associated journal publication. Following 3D reconstruction of the histological volumes and spatial normalisation into a common template space (cf. above) as described in detail in Amunts *et al.*, 2004, the individual maps of structures in the different brains are superimposed to create probabilistic maps. These maps describe how likely it is that a particular structure is found at each voxel of the reference space. Finally, as a summary of these individual maps into a distinct whole-brain parcellation, a Maximum Probability Map is computed, which assigns each voxel in the brain to the most likely histological area in that particular position (Eickhoff *et al.*, 2005, 2006).

¹ <http://help.brain-map.org/display/api/Atlas+Drawings+and+Ontologies>



2.2 Numbers and Distributions of Neurons and Glia (DeFelipe, UPM)

2.2.1 Data Description

We have started to characterise the density and principle patterns of spatial distribution of neurons and glia (DAPI nuclei of NeuN-positive and NeuN-negative neurons) in different human brain regions. We have processed material from autopsy brains with different *post mortem* periods and fixation procedures, in order to optimise and standardise protocols, and to establish how these factors might affect receptor binding and immunocytochemical experiments. We developed the procedures to perform the fixation in thin histological sections adjacent to those used for receptor binding experiments (unfixed tissue). Thereafter, we performed immunocytochemical stainings in large brain sections (whole hemisphere) in order to analyse multiple brain regions in single sections, which is critical for comparison with the receptor maps of adjacent sections generated in the laboratory of Karl Zilles and Katrin Amunts (*Heinrich Heine Universität Düsseldorf* [UDUS]). These tests showed, however, that the quality of the *post mortem* tissue is not yet good enough to perform quantitative analyses.

Therefore, we have focused on studying the density of different types of cells in brain tissue processed with another protocol. Specifically, we have used sections obtained from brain tissue that has been fixed in paraformaldehyde immediately after removal and with *post mortem* times of 2-3 hours. This tissue has been processed to allow use of immunocytochemistry to study the density and physical distribution of different types of cells (NeuN, PV, CR, CB, TH neurons), and axon terminal specialisations (chandelier and Double bouquet cell axon terminals and Complex Basket formations).

The cortical regions examined included the following Brodmann's cytoarchitectonic subdivisions: 1, 3b, 4, 6, 9, 10, 11, 12, 13, 14, 17, 18, 20, 21, 22, 24, 32, 38, 45, 46, 47 from three male individuals (aged 23, 49, and 69). The information was extracted as raw data to be shared with team from the École Polytechnique Fédérale de Lausanne (EPFL) for the purpose of building the registration pipelines. Part of this material has been obtained from previous work performed in DeFelipe's lab.

The data is provided as a set of Excel sheets, according to the following table:

Cell/Axon terminal type	human	age	gender	cortical region (Brodmann's area)	layer	staining	sampling method	file	reference
NeuN	M1,M7,M8	(23,49,69)	M,M,M	17,18,4,9,21,24	I,II,III,IV, V,VI	NeuN (DAB)	Disector	NeuN cell density.xls	Inda <i>et al.</i> , 2006
PV neurons	M1,M7,M8	(23,49,69)	M,M,M	9,10,11,12,13,14,17,18,20,21,22,24,32,38,45,46,47,1,3b,4	III	PV (DAB)	Disector	PV density.zip	not published
CR neurons	M1,M7,M8	(23,49,69)	M,M,M	9,10,11,12,13,14,17,18,20,21,22,24,32,38,45,46,47,1,3b,4	III	CR (DAB)	Disector	CR density.zip	not published
TH neurons	M1,M7	(23,49)	M,M	6,9,10,11,12,17,20,21,24,32,46	I-VI	TH (DAB)	N. of cells/mm ²	TH density.xls	Benavides-Piccione and DeFelipe 2007
Chandelier cell axon terminals	M1,M7,M8	(23,49,69)	M,M,M	9,10,11,12,13,14,17,18,20,21,22,24,32,38,45,46,47,1,3b,4	I,II,III,IV, V,VI	GAT-1 (DAB)	N. terminals/mm ²	Ch terminals.xls	Inda <i>et al.</i> , 2006
Complex Basket formations	M1,M7,M8, M14,M16	(23,49,69,59,40)	M,M,M, M,M	9,10,11,12,13,14,17,18,20,21,22,24,32,38,45,46,47,3b,4	I,II,III,IV, V,VI	VGAT (DAB)	N. of complex basket formations/mm ²	Complex Basket Formations.xlsx	Blazquez-Llorca <i>et al</i> 2010

Table 1: Provision of data on different cell types in different cortical areas.

2.2.2 Data Provenance

The data were obtained using human brain tissue from two sources: the laboratory of Katrin Amunts and the Forensic Pathology Service of the Basque Institute of Legal Medicine, Bilbao, Spain. Furthermore, DeFelipe's lab has access to a bank of human brain tissue—the *Banco de Tejidos Fundación CIEN*™ (BTFC; *Centro Alzheimer, Fundación Reina*



Sofía, Madrid, Spain), with which DeFelipe's lab has a long-lasting collaboration agreement. The BTFC makes healthy brain control samples available, as well as Alzheimer's disease brain samples. Following an evaluation of the clinical history and biosafety aspects of the case, a neuropathological autopsy is performed and the brain removed.

2.3 High resolution whole brain volumetric data; BigBrain (Mohlberg, JUELICH)

2.3.1 Data Description

The BigBrain dataset is a key element of the HBP Human Brain Atlas, representing a structural representation of the cytoarchitectonic of the human brain with the highest isotropic resolution currently available. So far, the dataset has been used in two cytoarchitectonic mapping projects. From these two projects the Te1.0, Te1.1, Te1.2, Te2.1, Te2.2, Te3, T11, T12, and TPJ cortical subregions of the auditory cortex were transformed into BigBrain space. To do this, the border information was measured and extracted in successive stained histological sections of the original distorted dataset, at a layer distance of up to 0.3mm as contour line data. We computed new linear and nonlinear transformations from the original distorted sections to the final repaired and corrected sections of the 3D reconstructed BigBrain dataset, because it would have been much more complicated—and thus error-prone—to combine the large number of individual transformations which have been computed for the original 3D reconstruction of the BigBrain. The newly computed transformations were applied to the contour line data, quality controlled, and shared with the EPFL team for the purpose of integrating the delineations of the auditory cortex into the BigBrain viewer of the Collaboratory.

In addition, efforts were carried out to achieve a match of the ontologies used for the cytoarchitectonic JuBrain atlas and the Collaboratory/Unified Portal data.

2.3.2 Data Provenance

The cytoarchitectonic delineations of the auditory cortex are based on observer-independent histological mapping performed in the stained histological sections of the first BigBrain dataset at an in-plane resolution of 1 μ m. The delineations were transferred to the reconstructed histological sections at a resolution of 20 μ m. Details of the histological processing and 3D reconstruction of the BigBrain dataset have been extensively described in Amunts *et al.*, 2012, and the approach for observer-independent delineation of brain regions is summarised in several peer-reviewed publications [Zilles *et al.*, 2002; Schleicher *et al.*, 2005].

2.4 Morphologies of selected neurons (Mansvelder, VU)

2.4.1 Data Description and Provenance

To populate models of synapses, neurons and networks of neurons in the human brain with accurate morphological and physiological parameters of human neurons, data from neuronal recordings are being exchanged continuously between Partners in SP2 (Mansvelder, Vrije Universiteit Amsterdam [VU]) and in SP4 and SP6 (Segev, Hebrew University of Jerusalem [HUJI]). A reference data set with digitally reconstructed neurons with matching physiological data from these neurons was provided by Mansvelder and used by Segev to model single neuron properties. Morphologies and physiologies of synaptically connected neuron pairs have also been exchanged. Using feature extraction, active properties of dendrites and axons of different types of neurons are currently being established (Eyal *et al.*, 2014)



2.5 Quantitative Receptor data (Zilles, JUELICH)

2.5.1 Data Description

We have labelled sections of human brains with up to 23 different receptor ligands. From this sample, we have defined a core set of fifteen ligands, which cover major receptor types of classical neurotransmitters (glutamate, GABA, acetylcholine, serotonin, noradrenalin and dopamine) as well as adenosine. The actual receptors studied up to now are: AMPA, NMDA, kainate, mGluR2/3, GABA_A, GABA_A associated benzodiazepine binding sites, GABA_B, muscarinic M₁, M₂ and M₃, nicotinic $\alpha 7$, $\alpha 5$, $\alpha 3$, $\beta 2$ 5-HT_{1A}, 5-HT_{2A}, D₁, A₁. Additionally, the D₂ and A_{2A} receptors, as well as antagonistic binding sites of the GABA_A and M₂ receptors, were labelled in some brains. Measurements were performed well ahead of the Milestone in three primary sensory, the primary motor, 11 higher associative cortical areas, putamen, globus pallidus and two thalamic nuclei (see table).

The dataset is provided as an Excel sheet, and attached in of this report. It is also provided to SP5 (Annex D).

2.5.2 Data Provenance

The methods about the provenance and processing of the data are described in Zilles *et al.* (2002). For further information on the provenance of the brains see Zilles *et al.* (2015).

2.6 *In vivo* fibre tract scans and diffusion-based data on major and U-shaped tracts (Mangin, Poupon, CEA)

2.6.1 Raw MRI data description

The CONNECT/Archi database described here was acquired on a Tim Trio 3T MRI system (Siemens, Erlangen) equipped with a whole body gradient set (40mT/m, 175 T/m/s) and a 12-channel head coil. It was aquired at Neurospin on 80 young healthy subjects (24 5 year old) in the frame of the European FP7 CONNECT project (PIs: C. Poupon, J.-F. Mangin), including structural and functional MRI data collected from three imaging sessions of 1 hour 30 minutes each.

The imaging protocol was approved by the Local Ethical Committee, corresponding to two separate ethical approvals (CPP100002 & CPP100022, Principal Investigator Dr Denis Le Bihan).

The structural MRI sessions include the acquisition of:

- 3 standard T1-weighted MRI scans (millimetre isotropic resolution and 0.75 mm isotropic resolution).
- 1 high resolution T1-weighted MRI scan (0.75 mm isotropic resolution).
- 2 single-shell HARDI (High Angular Resolution Diffusion Imaging) diffusion-weighted, twice refocused echoplanar MRI scans along 60 orientations, with two different diffusion sensitisations of $b=1500$ s/mm² and $b=3000$ s/mm².
- 1 multiple-shell diffusion-weighted twice-refocused echoplanar MRI scan along 20 orientations with 10 b-values between 0 and 3000 s/mm².
- 3 quantitative inversion recovery spin-echo / simple spin echo / gradient echo echoplanar MRI scans enabling the inference of T1, T2 and T2* relaxation times quantitatively.

The functional MRI session includes the acquisition of:

- 1 resting-state functional MRI scan (10 minutes, 3 mm isotropic resolution, 2.4 s repetition time)



- 1 'localizer' functional MRI scan including a series of visual, auditory, motor, mental arithmetic stimuli (10 minutes, 3 mm isotropic resolution, 2.4 s repetition time)
- 1 'social' functional MRI scan including a series of stimuli activating functional networks involved in social interactions (10 minutes, 3 mm isotropic resolution, 2.4 s repetition time)
- 1 'emotional' functional MRI scan including a series of stimuli activating functional networks involved in emotion processing (10 minutes, 3 mm isotropic resolution, 2.4 s repetition time)
- 1 'spatial' functional MRI scan including a series of stimuli activating functional networks in charge of spatial encoding (10 minutes, 3 mm isotropic resolution, 2.4 s repetition time).

For each session, a further B0 field mapping was performed using a double gradient echo MRI scan, to correct the geometrical distortions induced by susceptibility effects corrupting the echoplanar scans.

All individual pre-processed MRI scans (including the correction of all imaging artefacts using the Connectomist toolbox developed at Neurospin) will be delivered using NIFTI format. Functional MRI onsets will be delivered using Python dictionaries. Lastly, further information about subjects (age, weight, height, handedness) will be provided in CSV format.

2.6.2 Individual tractograms, quantitative maps, bundle maps and bundle density maps

After being pre-processed, all the subjects were processed with the Connectomist toolbox, using the following pipelines:

- Extraction of individual Q-space information, preparation of diffusion MRI data and construction of a rough mask of the brain.
- Computation of individual robust domains of propagation for tractography based on the segmentation of T1-weighted MRI data.
- Computation of individual fields of local HARDI models (here, the analytical Q-ball model with a spherical harmonics order 6 and a regularisation factor of 0.006 was chosen).
- Computation of individual tractograms inferred from former field of analytical Q-balls and using a streamline regularised deterministic fibre tracking algorithm.
- Extraction of individual fibre clusters from the former individual tractograms, using the robust clustering approach of Guevara *et al.*
- Segmentation of individual long and short white matter bundles using Guevara's atlas.
- Computation of individual probability density maps for all the long and short white matter bundles.

In the frame of SP2 Deliverables, we provide:

- The **individual tractograms** containing the whole set of individual tracked streamlines in the two **BrainVISA** and **VTK** formats. Documentation will describe the two formats.
- The **individual long and short white matter bundles** using the two **BrainVISA** and **VTK** formats, including the well-known long white matter bundles: Arcuate, Arcuate Anterior, Arcuate Posterior, Cingulum Long, Cingulum Temporal, Cingulum Short, Cortico-Spinal Tract, Fornix, Inferior Fronto-Occipital, Inferior Longitudinal, Uncinate, CorpusCallosum Rostrum, Corpus Callosum Splenium, Corpus Callosum Genu, Corpus Callosum Body, Thalamic Radiations Anterior, Thalamic Radiations Posterior, Thalamic Radiations Motor, Thalamic Radiations Parietal, Thalamic Radiations Inferior.



- The **individual probability density maps** of all the long and short white matter bundles in NIFTI format.
- Some **individual quantitative diffusion maps**, including FA, ADC, parallel and transverse diffusivities in NIFTI format.
- The **individual quantitative relaxometry maps** of T1, T2 and T2* relaxation times in NIFTI format.



Figure 2: Segmentation of the long white matter bundles obtained for all the subjects of the CONNECT/Archi database.

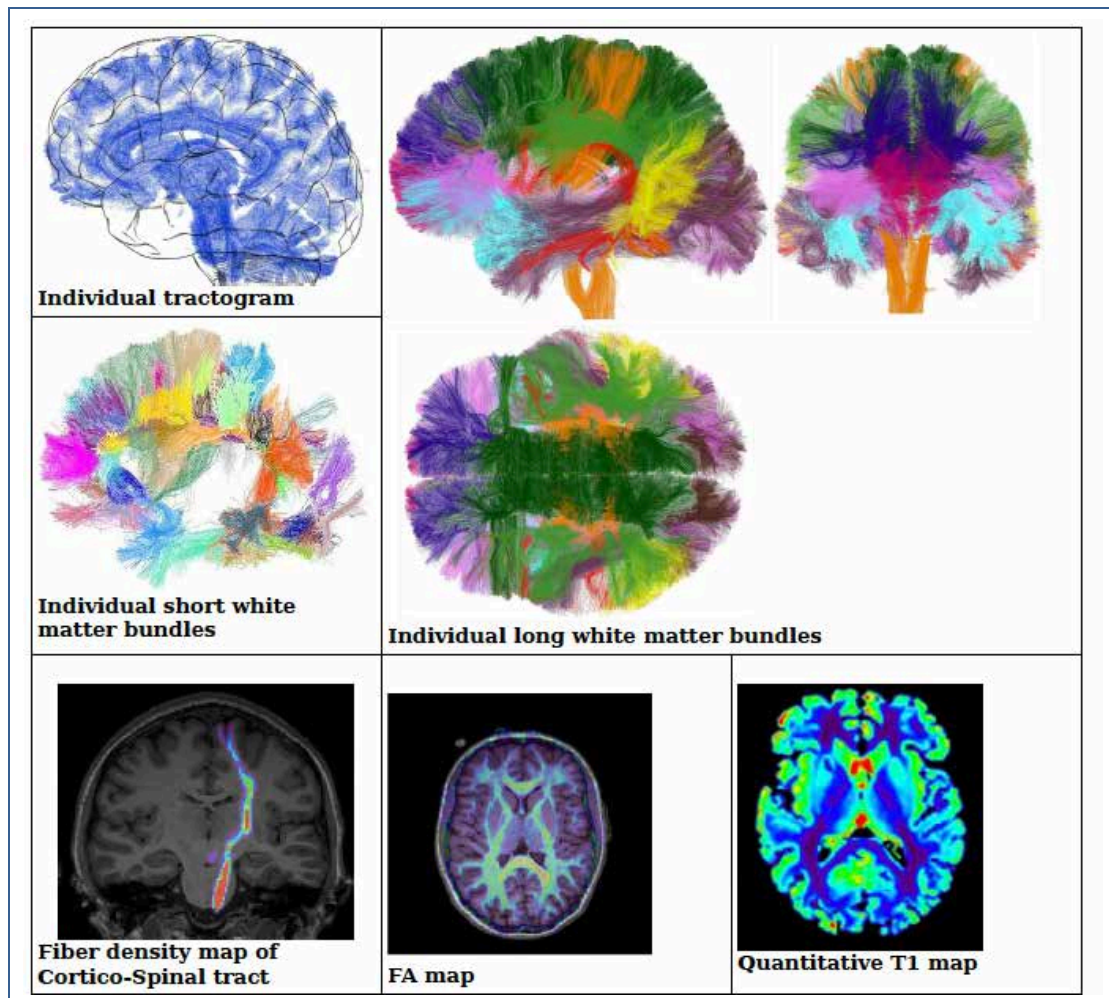


Figure 3: Examples of individual tractograms, segmented long and short white matter bundles, density map, quantitative diffusion map, and quantitative T1 relaxation time.

2.6.3 Atlas of long and short white matter structural connectivity

In the frame of SP2 Deliverables, we provide two diffusion-based connectivity atlases in the frame of MNI-ICBM152nlin2009casym:

- The atlas of long white matter bundles using BrainVISA and VTK formats
- The atlas of short white matter bundles using BrainVISA and VTK formats.

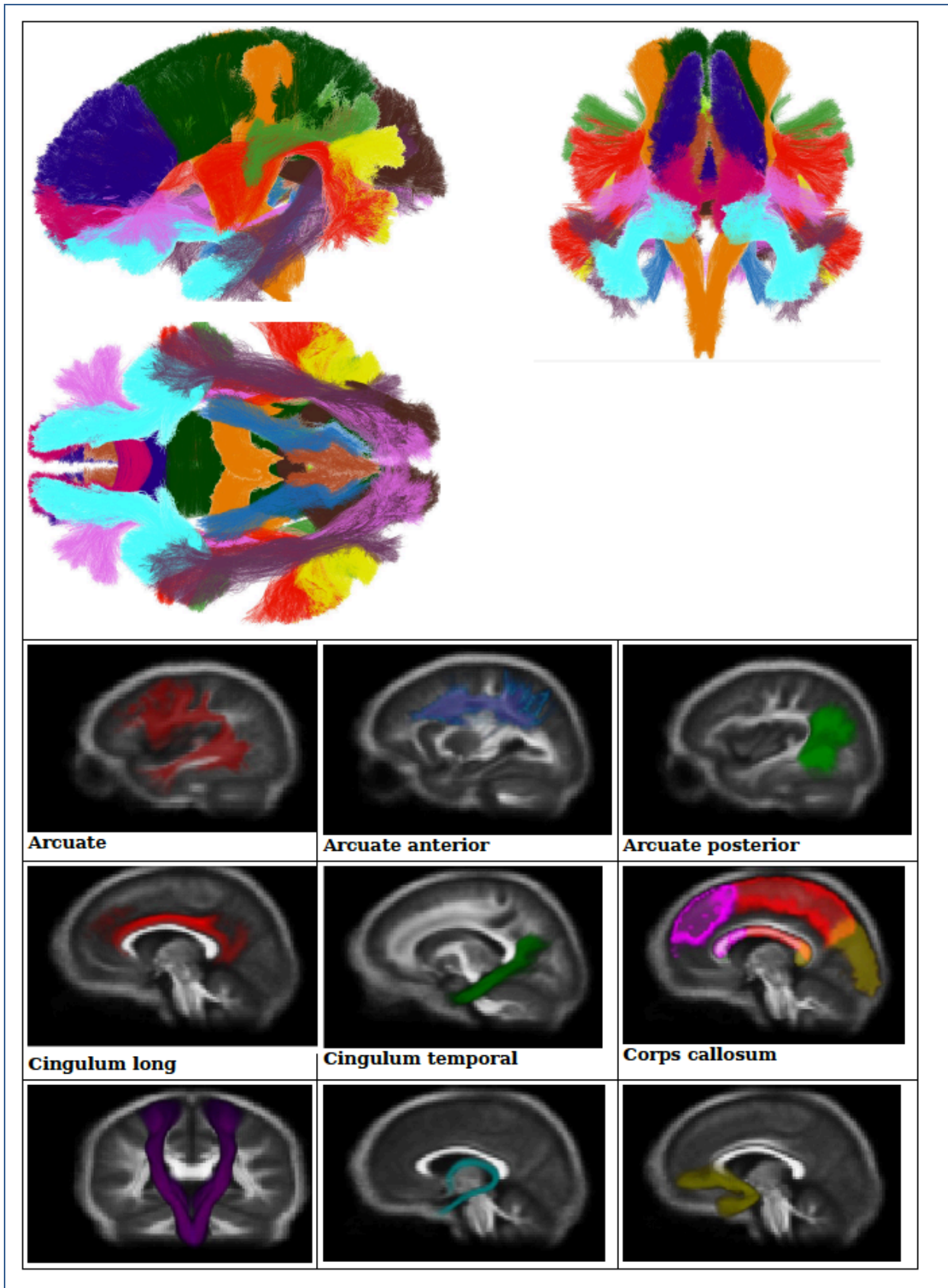
These atlases were computed from several pipelines of the Connectomist toolbox, starting from the intra-subject fibre clustering performed at the individual scale.

In addition, we also provide:

- The atlas of probability density maps of all the long and short white matter bundles in NIFTI format
- The atlas of quantitative diffusion maps including FA, ADC, parallel and transverse diffusivities in NIFTI format.

Depending on the status of the work in progress, we may also provide:

- The atlas of quantitative relaxometry maps of T1, T2 and T2* relaxation times in NIFTI format.



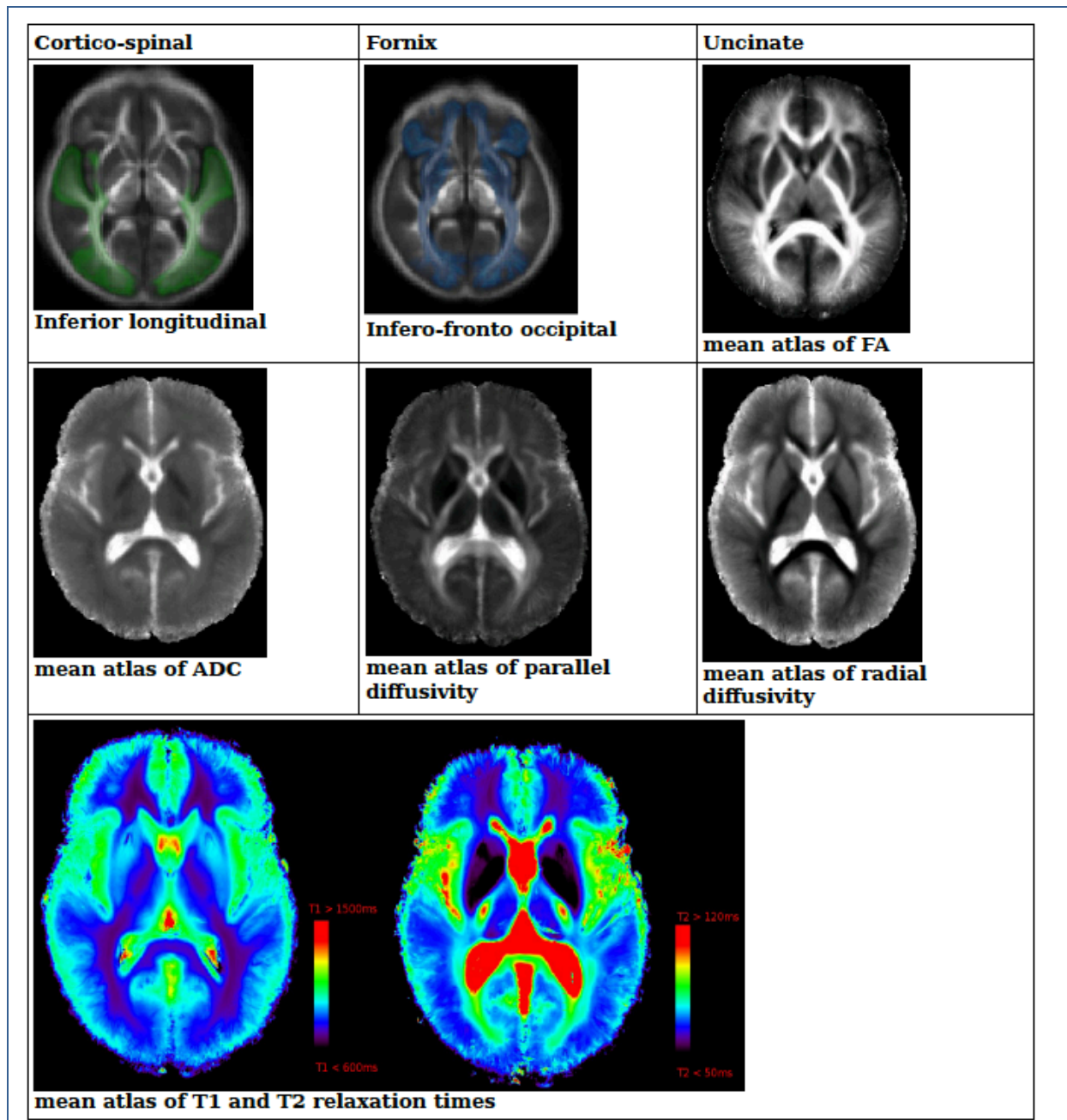


Figure 4: Representation of the atlas of long white matter connectivity merging the fibres of all the subjects, and example of bundle probability density maps, as well as atlases of quantitative diffusion and relaxometry indices.

2.7 Wistar rat brain fibre orientation model (Axer, Schubert, JUELICH)

2.7.1 Data Description

The 3D fibre orientation model of a Wistar rat brain was derived from 3D-Polarized Light Imaging (3D-PLI) as described in Axer *et al.* (2011a).

The Wistar rat brain was immersion fixed in 4% paraformaldehyde. After cryoprotection (20% glycerin), the brain was deep frozen at -70°C and stored till further processing. The brain was serially sectioned in the coronal plane (section thickness $60\ \mu\text{m}$) using a large-scale cryostat microtome (Polycut CM 3500, Leica, Germany) and coverslipped with glycerin. Immediately after coverslipping, the sections were measured using the large-area polarimeter (LAP, pixel size: $64\ \mu\text{m} \times 64\ \mu\text{m}$, cf. Axer, 2011a). During sectioning, each blockface was digitised using a CCD camera mounted above the brain in order to obtain an undistorted reference image of each section. No staining was applied. This procedure resulted in an uninterrupted series of sections through the entire brain, which ultimately enabled the 3D reconstruction.

The application of the Jones calculus [Jones, 1941] describes the light transmittance through the LAP and enables the calculation of the individual spatial fibre orientation in each voxel (defined by pixel size and section thickness). The fibre orientation is defined by the pair of angles $(\alpha, \phi) = (\text{inclination, direction})$, indicating the fibre axis orientation out of and within the section plane, respectively. Inclination and direction angles are encoded in HSV colour space to provide one fibre orientation map (FOM) per section. The entire data set of aligned FOMs (i.e. the fibre orientation model) is assembled in a single NIfTI file (<http://nifti.nimh.nih.gov>).

3D reconstruction of the FOMs was carried out in a sequential application of affine and b-spline based image alignment steps, with the reconstructed blockface volume acting as reference brain. Afterwards, the fibre orientation model was transferred into the common rodent reference space, the Waxholm Space atlas [Papp *et al.*, 2014]. The transformation of the brains into the same space was done in two steps: (i) a 3D affine registration ensured the correct spatial alignment of the brains, and (ii) a subsequent 3D non-linear registration compensated non-linear distortions of the brain sections.

The fibre orientation model of the rat brain is not part of the proposed deliverables, but it is of utmost relevance for cross-SPs data integration and platform developments.

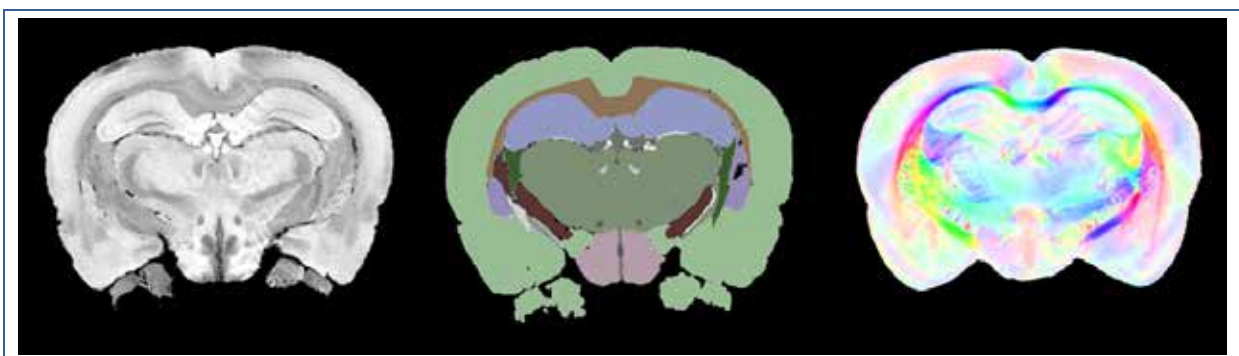


Figure 5: Example of the T2* image (left), the delineated atlas image (middle), and the fibre orientation map (right) of a coronal rat brain section in the same sectioning plane.

2.7.2 Data Provenance

The application of polarisation microscopy to unstained sections of brain tissue has been extensively described in peer-reviewed publications (e.g., Axer *et al.* 2011a,b, Larsen *et al.* 2007, Wiese *et al.* 2014). The 3D reconstruction of histological sections based on a blockface reference has been demonstrated by Palm *et al.* (2010). The Waxholm Space



atlas [Papp *et al.* (2014)] defines the reference space for rodents in the HBP. It consists of high resolution, contrast enhanced structural (including T2 and T2*-weighted) and diffusion weighted MR images with 39 μm isotropic voxels for the MRI volume, and 78 μm isotropic voxels for the DTI volume. In total, 76 major anatomical structures were delineated based on the architectural details in both grey and white matter, which were demonstrated by the structural images.

2.8 Whole rat brain receptor data (Schubert, Zilles, JUELICH)

2.8.1 Data Description

Transmitter receptors are key molecules of signal transmission. They are heterogeneously distributed throughout the brain. Therefore, in order to understand the anatomical and molecular organisation of the brain, it is necessary to analyse their spatial organisation and the relationship between regional and laminar receptor densities with defined anatomical structures. Quantitative *in vitro* receptor autoradiography is a well-established technique for demonstrating receptor binding sites at a high spatial resolution.

2.8.2 Data Provenance

The deep frozen rat brain was serially sectioned. Before the sectioning, a blockface image was acquired for every section. Alternating sections were processed for receptor binding sites (Zilles *et al.*, 2002) or for the visualisation of cell bodies (cell body stain after Merker 1983). Radiolabelled sections were exposed against tritium-sensitive films together with plastic scales of known radioactivity concentrations. The ensuing autoradiographs were digitised, and the density of receptor binding sites could be measured densitometrically (fmol/mg protein) in regions of interest.

During the processing of the sections, non-linear deformation artefacts occur and the spatial correlation between the brain sections gets lost. To obtain correct 3D information of the neuronal structures and receptor densities across the whole brain, the brain sections were 3D-reconstructed. Therefore, the blockface images were aligned (details in Schober *et al.* 2015) and used as 3D reference volume for the reconstruction of histologically stained or autoradiographically processed sections (details in Schubert *et al.* 2015, Huynh *et al.* 2015) (Fig. 6).

The dataset comprises the following files:

- 1) R8_reco_blockface.nii: reconstructed blockface volume
- 2) R8_reco_histology.nii: reconstructed histology volume
- 3) R8_reco_receptor_m2.nii: reconstructed autoradiography volume for the M2 receptor (fmol/mg protein).

To compensate for non-linear distortions, the reconstructed volumes were aligned with an undistorted reference volume, the common rodent reference template: the Waxholm Space atlas (Papp *et al.*, 2014). This procedure required three steps. First, a 2D alignment was carried out, where a few sections of the one brain were manually anchored into the other, so that the brains had the same orientation. Then, a 3D affine registration served as pre-registration for the subsequent 3D non-linear registration. Alignment of data to the Waxholm space was done in collaboration with SP5 (Jan Bjaalie).

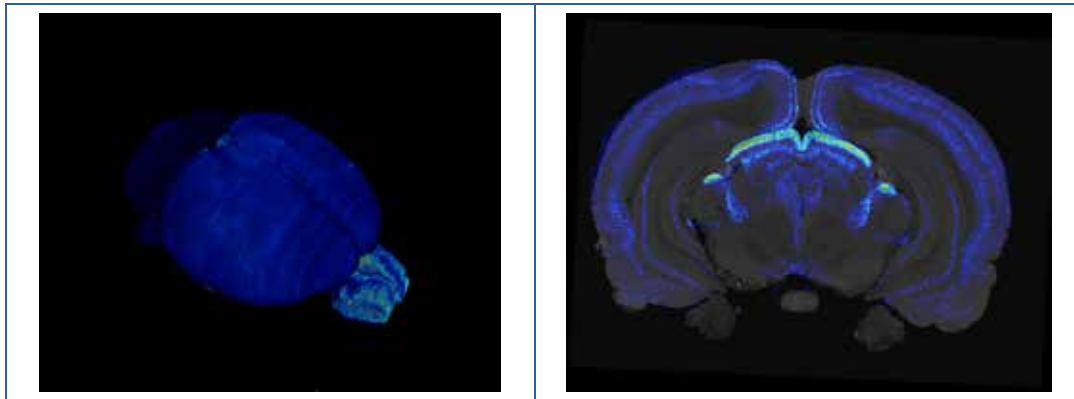


Figure 6: This 3D model in the stereotaxic reference space facilitates a multimodal voxel-wise analysis of the distribution of the receptors in 3D.

2.9 Infant atlas and major tracts in infant brains (Dehaene-Lambertz, CEA)

Our study on the maturational calendar of the linguistic pathways during the first six months of human life has been accepted (Dubois *et al.*, 2015, *Cerebral Cortex*, in press).

We now focus on the parcellation of the infant brain using grey and white matter maturational properties to specify the maturational sequence and its asynchrony across brain regions. As MRI parameters are sensitive to water molecules' environment and diffusion—they are affected by dendritic development and fibre myelination—we combined different MR sequences.

We first successfully developed a pipeline to correct the geometrical distortions induced by magnetic field inhomogeneities along the phase-encoding direction and by the large differences in magnetic susceptibility close to the interfaces (air/skull/brain), and to correctly realign the different MR sequences which are affected in a different way by these phenomena.

To then identify brain regions characterised by different microstructural and maturational properties, we performed clustering analyses on these parameters, without spatial priors, to localise regions of interest.

This analysis enabled us to easily visualise the progression of maturation within a specific brain region, with increasing age of infants and the maturation asynchrony across regions. The WM classes appear in “layers”: the maturation was observed from central to peripheral and from occipital to frontal regions. The GM classes highlight that the first mature regions were the primary cortical regions, and the last were in the parieto-occipital boundary and frontal lobe. These results are in agreement with *post-mortem* studies [Flechsig, 1920]. Further analyses will be conducted to perform clustering on GM and WM separately to confirm and refine our results.

The infant template is publicly available.

2.10 Human Intracranial Database (Lachaux, UCLB)

2.10.1 *Intermediate Report*

The Human Intracranial Database (HID) is a collection of intracranial EEG (iEEG) data from 30 patients, each performing eight functional localisers (eight short and classic paradigms designed to activate large-scale neural networks involved in language processing, verbal and visuo-spatial working memory, visual attention, motor behaviour, and high-level visual and auditory perception). 20 of those patients will also have fMRI data obtained during



localisers, including simultaneous fMRI/iEEG recordings. The HID also includes micro-recordings (micro-electrodes) during the localisers, and DTI/Cortico-Cortical Evoked Potentials connectivity measures (CCEP).

To date, the team is on track to provide the full data collection as scheduled by April 2016 (Month 30 Deliverable 2.3.4). We have acquired iEEG data from 25 patients during the localisers. Eight of the patients have been simultaneously recorded in iEEG and fMRI, and structural connectivity data has been acquired from six patients (DTI/CCEP). Micro-recordings began in February, following agreement from the ethical committee.

2.11 High-resolution optical imaging of human brain (Pavone, LENS)

2.11.1 Data Description

The *Laboratorio Europeo per la Spettroscopia Non-lineare* (LENS) developed two novel optical imaging apparatuses (one light sheet microscope and one serial two-photon microscope suited for cleared specimens) for the anatomical reconstruction of large brain areas with subcellular resolution and molecular specificity (immunofluorescence labelling). We modified the CLARITY protocol with the use of a cheap and versatile index-matching liquid (TDE). With the improved CLARITY technology and the serial two-photon microscope, we were able to image, without physically sectioning, a thick block of cortex from a hemimegalencephaly patient that was stained with different antibodies and cleared with TDE solution. We were able to label the tissue with a single antibody against parvalbumin (PV) or glial fibrillary acidic protein (GFAP) and DAPI, or with a combination of them. We could easily recognise single axons in the densely labelled sample, and trace them across the entire volume.

These data represent a preliminary study to demonstrate the possibility of studying millimetre-range projections in intact portions of brain tissue. The molecular specificity of the staining, and the high-throughput of the imaging methods, allow us to plan a systematic study of fine anatomy in selected brain regions. To this end, we are already preparing some samples from the labs of Katrin Amunts and Karl Zilles to study the distribution of muscarinic M2 receptors in different areas (V1 and motor cortex on Gyrus praecentralis).

Finally, together with collaborators in Florence, Rome and at the Allen Brain Institute, we developed some tools for the management and analysis of large image datasets. In particular, we devised software to stitch together terabyte-sized images, and to visualise them at multiple resolutions. We also developed a tool for the fully automatic localisation of cell somata in large volumes.

2.11.2 Data Provenance

The samples used for our preliminary tests on clearing and imaging technologies were kindly provided by the Meyer Paediatric Hospital in Florence.

3. Strategic Methods for the HBP Human Brain Atlas

3.1 Individual brain charting and meta-analysis (Thirion, INRIA)

The setting of an atlas of human brain function plays a key role in the HBP, as it will provide top-down constraints on the functional and structural organisation of future brain simulations. The available technology makes it possible to build such an atlas from measurements at the millimetre scale using non-invasive imaging (functional Magnetic Resonance Imaging, associated with Magneto-encephalography and other MRI

measurements). The Individual Brain Charting task is addressing this challenge, based on the combination of two strategies:

- 1) Gather and integrate all existing cognitive data into a model of brain functional organisation. For this, we have gathered all freely available data (Human Connectome Project, OpenfMRI, archi and NeuroVault; Gorgolewski *et al.*, 2015) into a consistent framework that links these data with relevant annotations. The crux is the statistical analysis of these data (meta-analysis, that relies on machine learning), which involves computational aspects (tractability of the learning procedures: Varoquaux *et al.*, 2013), sophisticated machine learning tools (supervised learning; Schwartz *et al.*, 2013, Thirion *et al.*, 2014b, Schwartz *et al.*, submitted) and statistical problems (model selection; Thirion *et al.*, 2014). The analysis of these data is currently bringing new insights on the network-level organisation of brain function (Bzdok *et al.*, submitted) and functional segregation of the brain (Schwartz *et al.*, submitted).

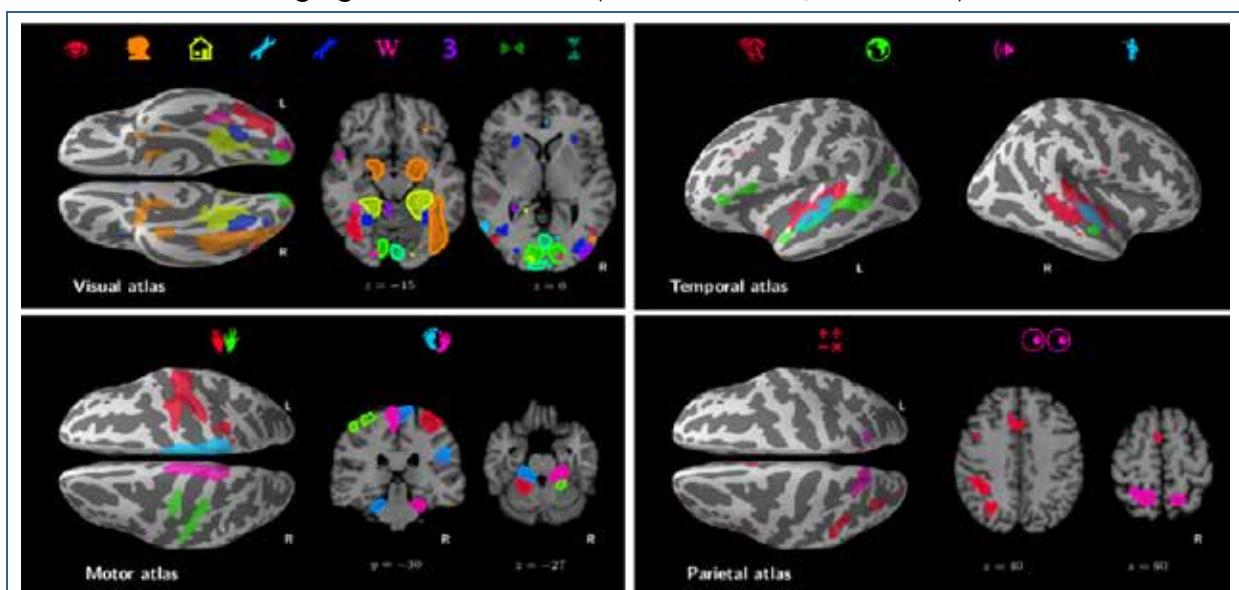


Figure 7: Applied to a corpus of 30 studies that we have gathered, our meta-analytic approach enables us to automatically and objectively map 20 cognitive terms. We report the corresponding regions for each concept in the above figure (Schwartz *et al.*, submitted).

- 2) Acquire new, better quality and higher resolution data to gain an order of magnitude in our description of brain functional circuits. This relies on us considering individual acquisition in a small group of subjects (12) that will be scanned in a vast amount of situations throughout the project (10 acquisitions during the Ramp-Up Phase). We are currently finalising the ethical and administrative aspects of this study, and running the first inclusion scans. In a pilot study (Thirion *et al.*, 2014a), we have already shown that an important fraction of cross-subject variability could be captured by the response to functional localiser experiments, showing that a sharper characterisation of brain function would be obtained by systematic intra-subject mapping.

The resources represented by these two approaches will be further developed and analysed jointly in the course of the project.

Our first Deliverable was the open-source Nilearn toolbox (<http://nilearn.github.io/release/0.1> in 01/2015), which provides the functions required to upload these data easily, organise them to enter machine learning analyses, efficiently perform various kinds of estimations, and write and visualise the results. Note that Nilearn relies on the reference Scikit-learn and joblib libraries developed by us and widely used by the HBP Neuroinformatics Platform.



3.2 SPM Anatomy Toolbox (Eickhoff)

The JuBrain Atlas Toolbox (a.k.a. "SPM Anatomy Toolbox") is a software program that allows the routine integration of structural and functional neuroimaging data with probabilistic cytoarchitectonic maps from the JuBrain atlas. Working at a 1 mm isotropic resolution that is comparable with *in-vivo* information, this toolbox provides several tools and measures for the allocation of *in-vivo* results to histological brain areas, and the construction of regions of interest from the JuBrain atlas. In the context of the HBP, the toolbox has been continuously expanded to cover new brain regions, and underwent a major revision in 2014 to increase compatibility with newer environments. It is currently available from the official website², and scheduled to be additionally distributed via the Neuroinformatics Platform.

3.3 A cross modality alignment toolbox based on sulci (Mangin)

Turning raw *post mortem* or *in vivo* acquisitions into maps of the human brain architecture requires cutting edge research and development in algorithmic methods and physics. Hence, most of the teams contributing to SP2 embed top-level methodologists among the leaders of the field. Some of the methods designed by the SP2 are part of HBP Deliverables, in addition to the "data". These methods can amount, for instance, to standardised acquisition protocols (tuning of the MRI scanner, etc.) or to software used to align or match an HBP Platform user's data with the HBP Atlas, in order to improve their analysis and finally contribute the data to the HBP data network.

During the Ramp-Up Phase, different software has been tuned to the HBP's needs, and will be embedded in the SP5 Neuroinformatics Platform in the future. These include:

- *Morphologist*, a pipeline dedicated to the automatic recognition of the cortical sulci in MRI data, has been adapted to *post mortem* and infant data. This pipeline, building upon a large number of algorithms, amounts to an artificial neuroanatomist developed over the last 20 years by the team of JF Mangin at Neurospin. Sulci provide a proxy of the localisation of the cortical architecture visible in any modality. Therefore, sulci are key features for aligning the numerous imaging modalities making the HBP atlas into a common referential (Mangin *et al.*, 2015).
- *Disco*, a pipeline aligning a set of brains using diffeomorphic transformations imposed by the matching of a set of sulci provided by Morphologist. This pipeline relies on the mathematical theory of current overcoming the difficulties induced by the variability of the sulci topologies. The versatility of this method has been increased to deal with the different modalities targeted by SP2, and also to support a research programme that aims to clarify the link between the cortical folding pattern and cortical architecture. The goal is to clarify the optima use of the sulci during alignment (Mangin *et al.*, 2015).
- *Connectomist-bundle*, a pipeline converting raw Diffusion MRI acquisitions into a large set of fibre bundles. This pipeline covers numerous pre-processing steps (distortion and motion correction), estimation of the diffusion models of the last generation, estimation of the tractogram of the complete white matter, and finally clustering and labelling of the streamline into bundles using the atlas provided to the HBP. These bundles will be used in the future to align any new diffusion data with the HBP space, using a bundle-based future release of Disco.

² http://www.fz-juelich.de/inm/inm-1/DE/Forschung/_docs/SPMAnatomyToolbox/SPMAnatomyToolbox_node.html



IBC-preprocessing: The preprocessing of the fMRI data used by the team of SP2 Partner Bertrand Thirion (*Institut national de recherche en informatique et en automatique* [INRIA]) for the Intensive Brain Charting project will be provided as a standard to be used for other datasets, before alignment with the IBC cortical parcellations. IBC pre-processing consists of Python code that relies on the open-source Nilearn, Nipype, Pyprocess and Nipy libraries. Future advanced functionalities (high-dimensional encoding, decoding, connectivity analysis, hyperalignment) will be based on the open-source Nilearn and Scikit-Learn libraries developed by the Parietal team.



Annex A: References

- Amunts K., Schleicher A., Bürgel U., Mohlberg H., Uylings H.B.M., Zilles K. (1999). Broca's region revisited: Cytoarchitecture and intersubject variability. *The Journal of Comparative Neurology* 412(2): 319-341.
- Amunts K., Weiss P.H., Mohlberg H., Pieperhoff P., Eickhoff S., Gurd J., Shah J.N., Marshall J.C., Fink G.R., Zilles K (2004) Analysis of the neural mechanisms underlying verbal fluency in cytoarchitectonically defined stereotactic space - The role of Brodmann's areas 44 and 45. *NeuroImage* 22(1): 42-56
- Amunts, K.; Zilles, K. (2012) Architecture and organizational principles of Broca's region (2012) *Trends in Cognitive Sciences* 16(8): 418-426. Doi: 10.1016/j.tics.2012.06.005
- Axer M., Amunts K., Grassel D., Palm C., Dammers J., Axer H., Pietrzyk U., Zilles K. (2011a) A novel approach to the human connectome: ultra-high resolution mapping of fiber tracts in the brain. *NeuroImage* 54:1091-1101.
- Axer M., Gräbel D., Kleiner M., Dammers J., Dickscheid T., Reckfort J., Hütz T., Eiben B., Pietrzyk U., Zilles K., Amunts K. (2011b) High-resolution fibre tract reconstruction in the human brain by means of three-dimensional polarized light imaging. *Frontiers in Neuroinformatics* 5:34.
- Biopreservation and Biobanking, (2012) Best practices for repositories collection, storage, retrieval, and distribution of biological materials for research international society for biological and environmental repositories. Vol. 10:79-161, 10(2):79-161. doi: 10.1089/bio.2012.1022.
- Bzdok D., Varoquaux G., Grisel O., Eickenberg M., Thirion B. Network-network architecture: Learning formal models from data. submitted.
- Dubois, J. *et al.*, 2015, *Cerebral Cortex*, in press
- Eickhoff S, Stephan KE, Mohlberg H, Grefkes C, Fink GR, Amunts K, Zilles K (2005):A new SPM toolbox for combining probabilistic cytoarchitectonic maps and functional imaging data. *NeuroImage* 25(4), 1325-1335
- Eickhoff, S. B.; Heim, S.; Zilles, K.; Amunts, K. (2006): Testing anatomically specified hypotheses in functional imaging using cytoarchitectonic maps. *NeuroImage* 32(2), 570-582
- Eickhoff SB, Paus T, Caspers S, Grosbras MH, Evans A, Zilles K, Amunts K (2007) Assignment of functional activations to probabilistic cytoarchitectonic areas revisited. *NeuroImage* 36(3), 511-521
- Eulenberg, P. zu; Caspers, S.; Roski, C.; Eickhoff, S.B. Meta-analytical definition and functional connectivity of the human vestibular cortex. 2012. *NeuroImage* 60:162-169.
- Eyal G, Mansvelder HD, de Kock CP, Segev I. (2014), Dendrites impact the encoding capabilities of the axon. *J Neurosci.* Jun 11; 34(24): 8063-71. doi:10.1523/JNEUROSCI.5431-13.2014. PMID: 24920612
- Flechsig (1920) *Anatomie des menschlichen Gehirns und Rückenmarks auf myelogenetischer Grundlage*, Verlag G. Thieme, Leipzig
- Genon *et al.*, in preparation
- Gorgolewski K.,Varoquaux G., Rivera G., Schwartz Y., Ghosh S.,Maumet C., Sochat V., Nichols T.,Poldrack R.,Poline J.-B., Yarkoni T., Margulies D. (2015) NeuroVault.org: A web-based repository for collecting and sharing unthresholded statistical maps of the human brain. *Frontiers Neuroinformatics*.
- Huynh A.-M., Kirlangic M.E., Schubert N., Schober M., Amunts K., Zilles K., Axer M. (2015) Reconstructing a Series of Auto-Radiographic Images in Rat Brains. *Procs. BVM*, 167-172
- Jones, R. C. (1941) A new calculus for the treatment of optical systems. *Journal of the Optical Society of America* 31, 488-493.
- Kabdebon, C., Leroy, F., Simmonet, H., Perrot, M., Dubois, J., Dehaene-Lambertz, G. (2014), Anatomical correlations of the international 10-20 sensor placement system in infants, *Neuroimage*,99C, 342-356.
- Larsen L, Griffin LD, Gräbel D, Witte OW, Axer H (2007) Polarized light imaging of white matter architecture. *Microsc Res Tech* 70:851-863.



- Mangin J.-F., Perrot M., Operto G., Cachia A., Fischer C., Lefèvre J. and Rivière D. (2015) Sulcus Identification and Labeling. In: Arthur W. Toga, editor. *Brain Mapping: An Encyclopedic Reference*, vol. 1, pp. 365-371. Academic Press: Elsevier
- Mangin J.-F., Auzias G., Coulon O., Sun Z.Y., Rivière D. and Régis J. (2015) Sulci as Landmarks. In: Arthur W. Toga, editor. *Brain Mapping: An Encyclopedic Reference*, vol. 2, pp. 45-52. Academic Press: Elsevier
- Martinez-Martin P., Avila, J. (2010) Alzheimer Center Reina Sofia Foundation: fighting the disease and providing overall solutions. *J Alzheimers Dis* 21: 337-348 doi: 10.3233/JAD-2010-101149.
- Merker B. (1983). Silver staining of cell bodies by means of physical development. *J Neurosci Methods* 9: 235-241.
- Palm, C., Axer, M., Gräßel, D., Dammers, J., Lindemeyer, J., Zilles, K., Pietrzyk, U., Amunts, K. (2010) Towards ultra-high resolution fibre tract mapping of the human brain - Registration of polarised light images and reorientation of fibre vectors. *Frontiers in Human Neuroscience* 4: 9: 1-16
- Papp, E.A. *et al.* (2014). Waxholm Space atlas of the Sprague Dawley rat brain. *NeuroImage*, 97: 374-386.
- Thirion B, Varoquaux G, Dohmatob E, Poline JB. (2014a) Which fMRI clustering gives good brain parcellations? *Front Neurosci.* Jul 1; 8:167.
- Thirion B, Varoquaux G, Grisel O, Poupon C, Pinel P. (2014b) Principal component regression predicts functional responses across individuals. *Med Image Comput Comput Assist Interv.*17(Pt 2):741-8.
- Schleicher, A.; Palomero-Gallagher, N.; Morosan, P.; Schleicher, S.B.; Kowalski, T.; de Vos, K.; Amunts, K.; Zilles, K. (2005) Quantitative architectural analysis: a new approach to cortical mapping. *Anat Embryol* 210: 373-386.
- Schober M., Schlömer P., Cremer M., Mohlberg H., Huynh A.-M., Schubert N., Kirlangic M.E., Amunts K., Axer M. (2015) Reference Volume Generation for Subsequent 3D-Reconstruction of Histological Sections. *Procs BVM*, 143-148
- Schubert N., Kirlangic M.E., Schober M., Huynh A.-M., Amunts K., Zilles K., Axer M. (2015) 3D Reconstruction of Histological Rat Brain Images. *Procs BVM*, 149-154
- Schwartz Y., Thirion B., and Varoquaux G. Brain data aggregation and function segregation, submitted.
- Schwartz Y., Thirion B., and Varoquaux G. Mapping cognitive ontologies to and from the brain (2013). In: *Advances in Neural Information Processing Systems (NIPS)*, Etats-Unis, November 2013.
- Sommer I.E.; Clos M.; Meijering A.L.; Diederer K.M.; Eickhoff, S.B. (2012) Resting state functional connectivity in patients with chronic hallucinations. *PLoS ONE* 7(9): e43516. Doi: 10.1371/journal.pone.0043516
- Wiese, H., Gräßel, D., Pietrzyk, U., Amunts, K. & Axer, M. (2014) Polarized light imaging of the human brain: a new approach to the data analysis of tilted sections. In: *Polarization: Measurement, Analysis, and Remote Sensing XI* (Eds. Chenault, D. B., Goldstein, D.H.). SPIE Vol. 9099, Bellingham.
- Varoquaux G., Schwartz Y., Pinel P., Thirion B. (2013) Cohort-level brain mapping: learning cognitive atoms to single out specialized regions. *Inf Process Med Imaging.*23: 438-49.
- Zilles, K., Schleicher, A., Palomero-Gallagher, N., Amunts, K. (2002) Quantitative analysis of cyto- and receptorarchitecture of the human brain, pp. 573-602. In: *Brain Mapping: The Methods*, 2nd edition (A.W. Toga and J.C. Mazziotta, eds.). Academic Press.
- Zilles, K., Bacha-Trams, M., Palomero-Gallagher, N., Amunts, K., Friederici, A.D. (2015) Common molecular basis of the sentence comprehension network revealed by neurotransmitter receptor fingerprints. *Cortex* 63: 79-89
- Zilles, K. *et al.* (2002). Quantitative analysis of cyto- and receptorarchitecture of the human brain, pp. 573-602. In: *Brain Mapping: The Methods*, 2nd edition (A.W. Toga and J.C. Mazziotta, eds.). San Diego, Academic Press.



Annex B: Data set Identification Card

Data set identification cards (DICs) will be required for each data set as part of the integration process. The metadata for the DICs will be collected and displayed online. While an online repository does not yet exist for these DICs, we present here the required criteria so that you can prepare the necessary information in advance:

- Name of the data set/software
- Description of the data/software: what data was generated or collected, what species, brain region (ontology for this defined by Neuroscience Information Framework NIF), cell type, origin (in vitro - post mortem), format (digital), size-scale
- Standards and metadata: Metadata provided in xml format according to Dublin Core Metadata Standard and others
- Access and sharing: Open or restricted access, identification of repository and its type. In case data sets cannot be shared the reasons should be mentioned (ethical, rules of personal data, privacy, security, IP, commercial) Where is the primary data located, what is the backup plan and the frequency, retention period
- Archiving and preservation: Procedure in place for long-term storage, indication how long data should be preserved, its approximate end volume, estimation of approximate costs for storage and preservation



Annex C: Receptor binding site densities for selected areas

Hierarchy / Function	Area	Stats	AMPA	Kainate	NMDA	GABA-A	GABA-B	BZ	M1	M2	M3	N	Alpha1	Alpha2	5-HT1A	5-HT2	D1
primary motor	4d	mean	282	310	701	1091	1434	1528	230	122	403	71	191	506	178	233	49
primary motor	4d	s.d.	93	111	155	397	1059	444	94	27	178	23	128	346	73	121	28
primary sensory	3b	mean	209	315	900	1490	1576	1938	327	196	456	50	184	961	153	377	85
primary sensory	3b	s.d.	122	153	195	490	706	694	90	46	365	30	55	356	72	102	21
primary sensory	Te1	mean	281	310	874	1187	1685	2071	386	214	255	60	201	672	153	299	108
primary sensory	Te1	s.d.	114	127	188	330	788	885	204	52	472	30	75	303	41	99	23
primary sensory	V1	mean	223	272	1183	2033	2163	1767	504	238	641	40	280	728	74	308	89
primary sensory	V1	s.d.	59	339	499	1148	945	1396	146	313	752	40	193	692	119	354	96
higher associative	44d	mean	316	337	990	1286	2033	2408	346	180	373	47	220	514	241	375	58
higher associative	44d	s.d.	186	117	196	143	489	665	103	89	451	40	59	303	58	134	38
higher associative	44v	mean	382	381	1085	1312	2039	2175	342	169	376	47	244	535	225	406	78
higher associative	44v	s.d.	195	145	308	134	606	655	165	67	446	40	73	289	64	140	31
higher associative	45a	mean	137	379	1331	1393	1972	2468	441	224	385	40	294	518	300	370	90
higher associative	45a	s.d.	191	160	636	211	308	252	51	95	269	26	44	369	73	74	9
higher associative	45p	mean	207	356	1021	1451	1697	2260	425	171	367	45	279	711	238	357	64
higher associative	45p	s.d.	150	140	241	120	605	434	63	108	327	23	76	169	59	152	23
higher associative	PF	mean	375	538	941	1490	2318	2224	543	164	766	47	307	159	230	402	103
higher associative	PF	s.d.	107	262	392	693	762	977	216	77	472	22	172	379	114	130	50
higher associative	PFcm	mean	443	339	1100	1304	1400	1890	541	141	356	29	277	534	185	327	107
higher associative	PFcm	s.d.	91	314	482	908	1106	1236	139	53	763	24	196	570	66	211	62
higher associative	PFm	mean	472	358	1088	1492	2418	2350	568	165	467	41	317	141	235	279	151
higher associative	PFm	s.d.	99	48	320	553	917	991	12	58	251	18	155	20	45	123	56



higher associative	PFop	mean	354	402	1109	1571	1860	2493	551	149	286	39	317	157	204	356	108
higher associative	PFop	s.d.	180	119	136	224	800	738	245	51	89	25	108	321	146	73	32
higher associative	P Ft	mean	396	436	1226	1627	1939	2439	501	200	286	37	331	392	197	348	95
higher associative	P Ft	s.d.	187	96	235	197	744	871	155	90	63	20	118	290	103	36	30
higher associative	PGa	mean	398	342	1014	1445	2451	1785	714	188	512	37	319	139	228	282	113
higher associative	PGa	s.d.	181	257	55	519	285	208	150	126	274	26	60	63	90	128	31
higher associative	PGp	mean	205	389	1009	1198	1780	1666	473	95	468	12	236	204	110	254	75
higher associative	PGp	s.d.	226	174	247	869	599	343	145	72	248	53	133	88	118	48	49
subcortical	putamen	mean	632	1332	869	788	1604	647	823	734	692	176	442	100	422	450	252
subcortical	putamen	s.d.	542	1753	398	507	1524	352	531	658	288	222	321	83	830	324	180
subcortical	globus pallidus	mean	98	115	439	92	247	426	119	30	175	17	250	55	32	148	53
subcortical	globus pallidus	s.d.	57	108	155	14	142	108	62	10	93	7	216	37	24	84	38
subcortical	anterior thalamic nucleus	mean	268	274	1084	539	2042	1053	179	663	271	192	1213	77	57	218	23
subcortical	anterior thalamic nucleus	s.d.	138	189	231	133	531	232	50	272	54	9	1083	60	32	127	8
subcortical	mediodorsal thalamic nucleus	mean	250	355	959	387	1992	1015	217	588	254	144	933	83	64	217	19
subcortical	mediodorsal thalamic nucleus	s.d.	141	292	229	101	889	47	123	228	41	24	764	57	40	129	3

Table 2: Cortical areas according to the JuBrain nomenclature and subcortical regions with mean \pm s.d. receptor binding site densities in fmol/mg protein in five adult human brains.



Annex D: JuBrain Ontology used in cytoarchitectonic atlas with direct relationship to Allen Brain Atlas

See attached file: [Zytoprojektliste_20150602_short.xls](#).